Published in final edited form as:
Cell Mol Life Sci. 2009 March ; 66(6): 1094–1104. doi:10.1007/s00018-009-8746-x.

Tauroursodeoxycholic acid prevents E22Q Alzheimer's Aβ toxicity in human cerebral endothelial cells

R. J. S. Viana[a], **A. F. Nunes**[a], **R. E. Castro**[a], **R. M. Ramalho**[a], **J. Meyerson**[b], **S. Fossati**[b], **J. Ghiso**[b,c], **A. Rostagno**[b], and **C. M. P. Rodrigues**[a]

[a]iMed.UL, Faculty of Pharmacy, University of Lisbon, Av. Prof. Gama Pinto, Lisbon 1649–019 (Portugal) Fax: +351-21-794-6491, cmprodrigues@ff.ul.pt

[b]Department of Pathology, New York University School of Medicine, New York, New York (USA)

[c]Department of Psychiatry, New York University School of Medicine, New York, New York (USA)

Abstract

The vasculotropic E22Q mutant of the amyloid-β (Aβ) peptide is associated with hereditary cerebral hemorrhage with amyloidosis Dutch type. The cellular mechanism(s) of toxicity and nature of the AβE22Q toxic assemblies are not completely understood. Comparative assessment of structural parameters and cell death mechanisms elicited in primary human cerebral endothelial cells by AβE22Q and wild-type Aβ revealed that only AβE22Q triggered the Bax mitochondrial pathway of apoptosis. AβE22Q neither matched the fast oligomerization kinetics of Aβ42 nor reached its predominant β-sheet structure, achieving a modest degree of oligomerization with a secondary structure that remained a mixture of β and random conformations. The endogenous molecule tauroursodeoxycholic acid (TUDCA) was a strong modulator of AβE22Q-triggered apoptosis but did not significantly change the secondary structures and fibrillogenic propensities of Aβ peptides. These data dissociate the pro-apoptotic properties of Aβ peptides from their distinct mechanisms of aggregation/fibrillization *in vitro*, providing new perspectives for modulation of amyloid toxicity.

Keywords

Apoptosis; cerebral amyloid angiopathy; E22Q mutant Aβ peptide; mitochondria; TUDCA

Introduction

Cerebral amyloid angiopathy (CAA), a common feature of Alzheimer's disease (AD), is an age-associated condition characterized by the deposition of amyloid peptides in cortical and leptomeningeal vessels, causing capillary disruption and endothelium dysfunction and playing a significant role in intra-cerebral hemorrhage [1–3]. Different proteins are associated with CAA (reviewed in [4,5]). The most common is amyloid-β (Aβ), which is the main component of the deposits seen in normal aging and sporadic AD that originates by processing of the amyloid precursor protein (APP) (reviewed in [6]). Of the several mutations identified in the APP gene, substitutions at residues flanking the Aβ region affect the rate of enzymatic APP processing and the production of Aβ42, resulting in an early-onset AD phenotype [7]. On the contrary, mutations within the Aβ sequence, particularly at residues 21 – 23, generate Aβ variants Dutch, Iowa, Flemish, Artic and Italian [8–11], which preferentially associate with

Correspondence to: C. M. P. Rodrigues.

CAA, hemorrhagic strokes and/or dementia. One of the most aggressive clinical phenotypes described in familial AD is associated with a glutamine to glutamic acid substitution at residue 22 (E22Q), found in a disorder known as hereditary cerebral hemorrhage with amyloidosis Dutch type (HCHWA-D) [8]. The disease is characterized by recurrent strokes and vascular dementia in the absence of neurofibrillar pathology, with fatal cerebral bleeding resulting from the massive amyloid deposition in leptomeningeal vessels and cortical arteries and arterioles (reviewed in [12]). Parenchymal mature plaques characteristic of AD are rare in this kindred, while diffuse preamyloid deposits are relatively frequent and show a remarkable relationship with age. They are more abundant in younger patients, suggesting that these lesions may develop into the less profuse mature fibrillar counter-parts [13–15].

In general, Aβ mutants have been demonstrated to exert stronger toxicity than the wild-type counterparts in both neuronal [16] and cerebrovascular cells [9,17–19], although striking differences exist among the variants themselves. Differences in toxicity likely correlate with distinct structural properties conferred by the amino acid substitutions, which typically translate into enhanced fibrillogenic properties [20,21]. These, in turn, influence the onset and aggressiveness of the respective clinical phenotypes (reviewed in [6]). One of the most-studied mutants is the aggressive intra-Aβ genetic variant E22Q. Following intraventricular injection in rats, this variant dramatically disrupts synaptic plasticity. Together with the Arctic (E22G) mutant, it is 100-fold more potent than wild-type Aβ40 at inhibiting long-term potentiation [22]. The Dutch Aβ peptide has also been shown to exert potent effects on vessel wall cells, exhibiting anti-angiogenic properties [23] and inducing apoptosis in cerebral endothelial and smooth muscle cells, under conditions in which wild-type Aβ had no effects [9,17–19]. Nevertheless, the cellular mechanism(s) by which Aβ mutants induce toxicity remains poorly understood and requires further investigation.

Tauroursodeoxycholic acid (TUDCA) is an endogenous bile acid known to play a key role in modulating the apoptotic threshold in various cell types by interfering with classical mitochondrial pathways of cell death [24]. Its antiapoptotic effects have been demonstrated in several pathological conditions, including different neurological disorders [25–29]. TUDCA modulates Aβ-induced cell death by inhibiting the mitochondrial pathway of apoptosis and enhancing survival signaling in rat cortical neurons [30]. Moreover, it can interfere with targets upstream of mitochondria, including cell cycle-related proteins E2F-1 and p53 [31], through functional modulation of nuclear steroid receptors [32]. These data strongly suggest that TUDCA may also be beneficial in reducing other manifestations of brain amyloid toxicity, such as CAA.

Many studies have been devoted to elucidate the mechanisms of Aβ neurotoxicity. However, there is limited information available regarding the effect(s) of amyloid peptides on endothelial vessel wall cells that are in immediate contact with the vascular amyloid deposits in CAA. In this study, we compared aggregation/fibrillization properties, secondary structure, and cell death pathways of the Dutch variant and wild-type Aβ40 and Aβ42, both in the presence and absence of TUDCA. Our data dissociate the apoptotic properties of Aβ peptides in human cerebral endothelial cells and their distinct mechanisms of aggregation *in vitro*, while providing new perspectives for modulation of amyloid-induced apoptosis.

Materials and methods

Peptide synthesis

Synthetic wild-type Aβ40 and Aβ42 peptides as well as Aβ40 peptide containing the E22Q substitution were synthesized by James I. Elliott at Yale University using *N-tert*-butyloxycarbonyl chemistry and then purified by reverse phase-high performance liquid chromatography on a Vydac C4 column (Western Analytical, Murrieta, CA) [9,33]. Molecular

masses were corroborated by matrix-assisted laser desorption ionization time-of-flight (MALDI-TOF) mass spectrometry, and concentration assessed by amino acid analysis. All peptides were supplied as single components eluted from the reverse-phase columns with experimental molecular masses of 4329.41 Da for Aβ40 (theoretical mass, 4329.86 Da), 4514.24 Da for Aβ42 (theoretical mass, 4514.10 Da) and 4328.80 Da for Aβ40E22Q (theoretical mass, 4328.87 Da).

Peptide aggregation

Synthetic Aβ homologues were dissolved to 1 mM in hexafluoro-isopropanol (HFIP; Sigma Chemical Co., St. Louis, MO), a pre-treatment that breaks down β-sheet structures and disrupts hydrophobic forces leading to monodisperse Aβ preparations [34]. Following lyophilization to remove HFIP, peptides were subsequently solubilized in deionized water and added to an equal volume of a 2× concentrated phosphate-buffered saline (PBS), pH 7.4, to a final concentration of 1 mg/ml in 1 × PBS. Peptides, in the presence or absence of 100 μM TUDCA (Sigma), were either incubated at 37°C for up to 48 h for the aggregation studies or diluted into culture media at the required concentration for the toxicity experiments. For the aggregation studies, structural properties were assessed by Western blot analysis, circular dichroism (CD) spectroscopy and Thioflavin T binding.

Peptide structural analysis

For the Western blot analysis, 200 ng aliquots of each peptide either freshly solubilized or after 24 and 48 h of aggregation, in the presence or absence of TUDCA, were separated on 16.5% Tris-Tricine SDS-polyacrylamide gel electrophoresis (PAGE). After electrophoresis, proteins were electrotransferred to nitrocellulose membranes (Hybond-ECL; GE Healthcare Life Sciences, Piscataway, NJ) using 10 mM 3-cyclohexylamino-1-propanesulfonic acid (Sigma) buffer, pH 11.0, containing 10% (v/v) methanol, at 400 mA for 2 h. After blocking in 5% nonfat milk in PBS containing 0.1%Tween 20, the membranes were immunoreacted with a combination of mouse monoclonal anti-Aβ antibodies 4G8 (epitope: residues Aβ18–22) and 6E10 (epitope: residues Aβ3 – 8), both from Covance (Princeton, NJ), at a 1/3000 dilution each, followed by incubation with horseradish peroxidase (HRP)-labeled F(ab′)2 anti-mouse IgG (1/5000; GE Healthcare Life Sciences). Fluorograms were developed with SuperSignal West Pico Chemiluminescent Substrate (Thermo Scientific, Rockford, IL) and exposed to Hyperfilm ECL (GE Healthcare Life Sciences).

The secondary structure of Aβ peptides was estimated by CD spectroscopy as previously described [9,33]. Spectra in the far-UV light (190 – 260 nm; bandwidth, 1 nm; intervals, 1 nm; scan rate, 60 nm/min) yielded by the different peptides at each time point of aggregation were recorded at 24 C with a Jasco J-720 spectropolarimeter (Jasco Corp., Tokyo, Japan), using a 0.2-mm-path quartz cell and a peptide concentration of 1 mg/ml. For each sample, 15 consecutive spectra were obtained, averaged and baseline-subtracted. Results were expressed in terms of mean residue ellipticity (degree-cm^2 dmol^{-1}) [35].

Thioflavin T binding was assessed essentially as previously described [36,37]. Six-microliter aliquots of each of the peptide aggregation time-point samples were added to 10 μl of 0.1 mM Thioflavin T (Sigma) and 50 mM Tris-HCl buffer, pH 8.5 to a final volume of 200 μl. Fluorescence was recorded after 300 s in a LS-50B luminescence spectrometer (Perkin Elmer, Waltham, MA) with excitation and emission wavelengths of 435 nm (slit width=10 nm) and 490 nm (slit width=10 nm), respectively. Each sample was analyzed in duplicate.

Culture of human brain microvascular endothelial cells

Primary human cerebral endothelial cells (HCEC; Cell Systems, Kirkland, WA) were grown in CS-C Complete Medium on dishes coated with Attachment Factor (Cell Systems), at 37°C

in a 5% CO_2 atmosphere. For cell death assays and immunocytochemistry, cells were plated at a density of 4×10^4 cells/ml. For immunoblotting, cells were plated at a density of 1×10^5 cells/ml. In all cases, cells were allowed to rest for 1 day prior to treatment with the Aβ peptides.

Induction of apoptosis

HFIP pre-treated Aβ peptides were dissolved to 500 μM in PBS, as indicated above, and subsequently added to warm F12K Nutrient Mixture (Invitrogen/Gibco, Carlsbad, CA) supplemented with 1%fetal bovine serum (FBS; Invitrogen/Gibco) to a 50 μM final concentration. These freshly prepared peptide solutions were incubated with HCECs, cultured as described above, for 12 or 24 h. In co-incubation experiments, 100 μM TUDCA was added to the cell cultures 12 h prior to the addition of Aβ peptides. As negative controls, cells were separately incubated either in the absence of amyloid peptides or with TUDCA alone. In all cases, attached cells were either fixed for Hoechst staining and immunocytochemistry analysis, or processed for viability assays. For Western blot analysis, attached and floating cells were combined prior to the preparation of cytosolic and mitochondrial protein fractions and subsequent protein extraction.

Measurement of cell death

Cell viability was measured by trypan blue exclusion and by the lactate dehydrogenase (LDH) viability assay (Sigma) according to the manufacturer's instructions. Apoptotic nuclei were detected by Hoechst labeling after cell fixation with 4% formaldehyde in PBS, for 10 min at room temperature. Following incubation with Hoechst dye 33258 (Sigma) at 5 μg/ml in PBS for 5 min, and PBS washes, slides were mounted with PBS:glycerol (3:1, v/v) and fluorescence visualized with an Axioskop fluorescence microscope (Carl Zeiss GmbH, Hamburg, Germany). Fluorescent nuclei were scored and categorized according to the condensation and staining characteristics of chromatin. Normal nuclei showed non-condensed chromatin dispersed over the entire nucleus. Apoptotic nuclei were identified by condensed and fragmented chromatin contiguous to the nuclear membrane, as well as nuclear fragmentation and presence of apoptotic bodies. Three random microscopic fields per sample of approximately 250 nuclei were counted and mean values expressed as the percentage of apoptotic nuclei.

Immunocytochemistry

After 24 h of exposure to the respective amyloid peptides, both in the presence and absence of TUDCA, HCECs were either directly processed for mitochondria labeling in live cells or fixed in 4% formaldehyde in PBS as above for the immunocytochemical evaluation of cytochrome *c* and Bax.

Staining of mitochondria in Aβ-challenged cells was performed by incubation for 30 min with 100 nM Red-Fluorescent MitoTracker Probe (Invitrogen/Molecular Probes, Eugene, OR) to allow for the selective incorporation of the dye and subsequent staining of the organelles. Immunofluorescence signals were evaluated using fluorescence microscopy as above. Bax mitochondrial immunocolocalization was performed with the Tyramide Signal Amplification Kit (Invitrogen/Molecular Probes), according to the manufacturer's instructions. Briefly, cells were fixed with 4% formaldehyde as above, washed with PBS and incubated with 1% blocking reagent, 0.1% Triton X-100 for 1 h, at room temperature. Incubation with mouse monoclonal anti-Bax antibody (Santa Cruz Biotechnology, Santa Cruz, CA) (1:50 in blocking solution; overnight, 4°C) was followed by HRP-conjugated goat anti-mouse IgG (Bio-Rad Laboratories, Hercules, CA) (1:200; 1 h, room temperature). Cells were subsequently incubated with Alexa Fluor 350-labeled tyramide (1:100 in amplification buffer/0.0015% H_2O_2 ; 10 min, room temperature), washed with PBS and mounted in PBS: glycerol (3:1, v/v). Fluorescence was visualized as above.

For cytochrome *c* immunostaining, after Aβ challenge and fixation, HCECs were incubated for 1 h with PBS containing 0.3% Triton X-100 (PBST) and 20 mg/ml bovine serum albumin (BSA). This was followed by 2 h incubation with monoclonal antibody anti-cytochrome *c* (BD Biosciences, Franklin Lakes, NJ; 1:200 in PBST containing 5 mg/ml BSA) and 1 h reaction with Alexa Fluor 488 conjugated anti-mouse secondary antibody (Invitrogen; 1:200 in PBST with 5 mg/ml BSA). Slides were mounted with Dapi-containing Mounting Medium (Vectashield, Burlingame, CA) and images acquired in a Nikon Eclipse E-800 Deconvolution Microscope, using Image-Pro Plus software (Media Cybernetics, Silver Springs, MD) and Autodeblur (AutoQuant Imaging, Inc., Watervliet, NY) for deconvolution. Specificity of immune detection was assessed by omission of the primary antibody.

Bax translocation and cytochrome *c* release

Subcellular distribution of Bax and cytochrome *c* in amyloid-challenged HCECs was determined using mitochondrial and cytosolic protein extracts. Briefly, cells were collected by centrifugation at 600 *g* for 5 min at 4°C. The pellets were washed once in ice-cold PBS and resuspended with 3 volumes of isolation buffer (20 mM HEPES/KOH, pH 7.5, 10 mM KCl, 1.5 mM $MgCl_2$, 1 mM EDTA, 1 mM EGTA, 1 mM DTT) supplemented with Complete protease inhibitor cocktail tablets (Roche Diagnostics GmbH, Mannheim, Germany), in 250 mM sucrose. After chilling on ice for 15 min, cells were disrupted by 40 strokes of a glass homogenizer, and homogenates were centrifuged twice at 2500 *g* for 10 min at 4°C to remove unbroken cells and nuclei. The supernatants were further centrifuged at 12 000 *g* for 30 min at 4°C, and the pellets containing the mitochondrial fraction resuspended in isolation buffer and frozen at −80°C. For cytosolic proteins, the 12 000 *g* supernatants were collected, filtered sequentially through 0.2 μm and 0.1 μm Ultrafree MC filters (Millipore, Bedford, MA) to remove other cellular organelles, and frozen at −80°C. Protein concentrations of the subcellular fractions were determined using the Bio-Rad protein assay kit according to the manufacturer's specifications. For Western blot detection of cytochrome *c* and Bax, typically 10 μg of mitochondrial and 50 μg of cytosolic proteins were separated on 15% SDS-PAGE and transferred onto nitrocellulose membranes. After sequentially blocking with 15% H_2O_2 and 5% non-fat milk (1 h, room temperature), membranes were separately incubated overnight at 4°C with mouse monoclonal anti-Bax (Santa Cruz Biotechnology) and anti-cytochrome *c* (PharMingen, San Diego, CA) diluted 1:500, and 1:2000, respectively. Finally, immunoblots were incubated with HRP-conjugated secondary antibodies (Bio-Rad Laboratories; 1:5000, 3 h, room temperature) and processed for chemiluminescence detection using the SuperSignal Chemiluminescent Substrate (Thermo Scientific). Mitochondrial contamination of the cytosolic protein extracts was assessed with cytochrome *c* oxidase II (Cox II; Santa Cruz Biotechnology; 1:200). Cox II and β-actin (Sigma; 1:25 000) were used as loading controls for mitochondrial and cytosolic fractions, respectively.

Statistical analysis

Statistical analysis was performed using GraphPad InStat version 3.00 (Graph-Pad Software) for the analysis of variance and Bonferroni's multiple comparison tests. Values of $p<0.05$ were considered significant.

Results

TUDCA does not affect Aβ peptide aggregation and secondary structure

It has been postulated that Aβ toxicity correlates with peptide aggregation propensity. Based on our previous findings demonstrating an inhibitory role of TUDCA on Aβ neurotoxicity, we studied its effect on the aggregation/fibrillization properties of the Dutch variant comparing with wild-type Aβ40 and Aβ42. As indicated in Figure 1a, wild-type Aβ40 remained mostly monomeric up to 48 h of incubation, with the appearance of only faint dimeric bands on Western

blot analysis at this time point. In contrast, as expected, Aβ42 showed high tendency to aggregate. Dimers and even faint tetrameric species were observed immediately after solubilization, whereas high molecular mass aggregates were readily visible at 24 h and accentuated at 48 h. AβE22Q showed an intermediate behavior with the formation of SDS-resistant oligomeric assemblies clearly noticeable at 48 h incubation but of lower molecular masses than those of Aβ42. Notably, in all cases, co-incubation with TUDCA resulted in no significant changes in the aggregation properties of the different peptides. The effect of TUDCA on the fibrillogenic propensity of the peptides was assessed by Thioflavin T binding. Co-incubation with TUDCA did not modify the inherent properties of each peptide (Fig. 1b). In fact, Aβ42 continued to express the highest fluorescence values, while Aβ40 levels remained negligible even at 48 h. AβE22Q showed an intermediate behavior, in agreement with the aggregation pattern shown in Figure 1a. Secondary structure analysis by CD spectroscopy illustrated both the different structural characteristics of the peptides and the lack of effect of TUDCA (Fig. 1c). The initial Aβ40 structure showed a minimum at 198 nm, characteristic of unordered conformations. Within 48 h of incubation, the peptide acquired Aβ-sheet-rich structure showing the typical minimum at 218 nm in the CD scan. Aβ42 showed a predominantly β-sheet conformation even immediately after solubilization. AβE22Q exhibited an intermediate structural configuration, in agreement with the data illustrated in Figure 1a and b, with a mixture of random and β-sheet components when freshly solubilized and an increase in the β-sheet component at 48 h. However, AβE22Q did not achieve the predominant β-sheet conformation of the Aβ42 in the time frame of the experiments. Corroborating the Western blot and Thioflavin T data, co-incubation with TUDCA-did not induce conformational changes in the secondary structures of any of the Aβ peptides studied.

TUDCA inhibits AβE22Q-induced apoptosis in brain microvascular endothelial cells

Morphologic evaluation of apoptosis induced by Aβ peptides in HCEC was performed by fluorescence microscopy following Hoechst staining (Fig. 2a). The results showed that nuclear fragmentation was differentially triggered by Aβ peptides, starting at 12 h of treatment, with a maximum at 24 h, under the conditions tested. Interestingly, the AβE22Q variant was very aggressive in HCECs, increasing apoptosis by almost threefold compared to controls ($p<0.001$), in contrast to wild-type Aβ40 and Aβ42, which had almost no effect (Fig. 2b). Consistent with its vasculotropic properties, AβE22Q did not significantly increase cell death in primary rat cortical neurons (unpublished observations). TUDCA was highly effective at modulating AβE22Q-induced toxicity, significantly inhibiting peptide-induced nuclear fragmentation to levels comparable to controls ($p<0.05$). Trypan blue dye exclusion and LDH levels (data not shown) were in accordance with the morphological results. Detailed characterization of the structural assemblies of AβE22Q indicated that the induction of apoptosis correlated with the presence of peptide oligomers of low molecular mass and intermediate Thioflavin-binding capacity (Fig. 1). Notably, pre-treatment with TUDCA did not induce significant changes either in the peptide structure or in the aggregation/fibrillization propensity.

TUDCA prevents AβE22Q-induced mitochondrial Bax translocation and cytochrome *c* release

To further investigate the cell death pathways differentially triggered by Aβ peptides in HCECs, we sought to determine the specific involvement of the mitochondrial pathway of apoptosis. Our results showed that the AβE22Q mutant was very effective at triggering cytochrome *c* translocation from mitochondria to the cytosol when compared to Aβ40 and Aβ42 (Fig. 3), which exhibited almost negligible effects. This is consistent with the lack of ability of the wild-type peptides to induce major apoptotic changes in HCECs. Data on Bax translocation from the cytosol to mitochondria, assessed by Western blot, were in agreement with cytochrome *c* changes (Fig. 3). The role of TUDCA in preventing AβE22Q-induced, mitochondria-

dependent cell death was assessed by immunofluorescence microscopy. We confirmed that incubation of HCECs with the AβE22Q mutant resulted in cytochrome *c* release from mitochondria as illustrated by strong cytoplasmic staining, which was mostly abolished by TUDCA (Fig. 4). In addition, our results demonstrated that TUDCA significantly reduced co-localization of Bax with mitochondrial markers after incubation of HCECs with AβE22Q (Fig. 5a). In fact, TUDCA reduced mitochondrial co-localization of Bax to control values (Fig. 5b; $p<0.05$).

Discussion

Extensive CAA is the neuropathological hallmark of familial AD cases linked to intra-Aβ mutations. These Aβ genetic variants show potent vasculotropic properties and result in a predominant deposition of Aβ peptides ending at position 40 [38–40]. These are also the species that target the vasculature in sporadic AD, in contrast with the primary association of Aβ42 with the parenchymal deposits [41,42].

Aggregation/fibrillization of Aβ plays a critical role in neurodegeneration. It is now considered that the transition from soluble monomeric species circulating under normal conditions to the oligomeric, protofibrillar and end-point fibrillar assemblies contribute significantly to disease pathogenesis. In particular, intermediate oligomeric and protofibrillar forms seem to display the most potent effects in neuronal cells, inducing synaptic disruption and neurotoxicity (reviewed in [43,44]). In contrast, the abundance of mature amyloid plaques correlates poorly with AD severity [45,46]. Mutants with accelerated formation of intermediate species and increased stability of these structures, such as the Arctic (E22G) variant, elicit an earlier and stronger effect on neuronal cells compared with wild-type peptides [21,47]. In contrast, the effect of Aβ genetic variants on cerebral vessel wall cells, specifically on endothelial cells, has not been so well characterized. The E22Q peptide has been shown to selectively exert deleterious effects on these cells, significantly increasing apoptotic responses in comparison to the wild-type Aβ40 [9,19]. Nevertheless, the nature of the amyloid assemblies inducing toxicity remains uncertain. In the present study, we characterized in detail the conformational properties of the E22Q peptide triggering apoptotic responses in HCECs and demonstrated its intermediate fibrillogenic/aggregation properties and content of β-sheet conformation compared with wild-type Aβ40 and Aβ42. At one extreme, Aβ40 exhibited a virtual lack of oligomerization; at the other, Aβ42 showed high molecular mass assemblies with strong fibrillar components. The absence of apoptosis resulting from endothelial challenge with both wild-type peptides suggests that the intermediate conformation of the E22Q oligomeric assemblies accounts for the potent, specific apoptotic effect of this genetic variant.

The limited high-order oligomerization/fibrillization observed in AβE22Q correlates well with the findings from nuclear magnetic resonance spectroscopy and molecular dynamics simulation studies, which highlight the effect of the mutation in fibril stabilization [48,49]. These studies indicate that the wild-type Aβ peptide, although mostly unstructured in solution, bears some regions exhibiting structural order and protease resistance. A fragment stretching from amino acids 21 through 30 adopts a stable bend structure which appears to nucleate monomer folding [50]. The turn is stabilized by hydrophobic interactions between Val24 and Lys28 and by long-range electrostatic interactions between Lys28 and either Glu22 or Asp23. The computational studies predicted that the E22Q mutation would translate into destabilization of the turn and enhanced oligomerization propensity [51,52], consistent with our findings. Also, a contributing factor to the nucleation propensity of the Dutch variant may be constituted by the depletion of the Glu22-Lys28 salt bridge as a consequence of the Glu-for-Gln substitution [52].

The major form of apoptosis in mammalian cells proceeds through the mitochondrial pathway, which involves mitochondrial outer membrane permeabilization and modulation by the Bcl-2 family of proteins. While some members of this family, typically located in the mitochondrial membrane, are potent inhibitors of apoptosis, others, including Bax, are pro-apoptotic and predominantly cytosolic (reviewed in [53]). Upon commitment to apoptosis, and after mitochondrial translocation, Bax undergoes conformational changes, oligomerizes and forms pores in the outer mitochondrial membrane, allowing the release of proteins, including apoptogenic cytochrome *c*, to the cytoplasm. These events facilitate downstream stages of the cell death cascades, leading to DNA fragmentation and formation of apoptotic bodies. Our data clearly demonstrate that AβE22Q is a strong inducer of the Bax pro-apoptotic mitochondrial pathway in HCEC and highlights its role in various downstream events. In fact, E22Q increased mitochondrial Bax and, consequently, cytosolic cytochrome *c*. As expected, both events were accompanied by downstream nuclear fragmentation. Although apoptosis indicators have not been investigated in HCHWA-D cases, it is noteworthy that studies in AD patients have demonstrated alterations in the expression of apoptosis-related genes, such as Bax [54,55], suggesting that this process also takes place *in vivo*.

TUDCA is an endogenous bile acid that modulates the apoptotic threshold by interfering with classical mitochondrial pathways of cell death [24]. It has been previously shown that TUDCA is neuroprotective in pharmacological and transgenic mouse models of Huntington's disease [27,56], reduces lesion volumes in rat models of ischemic and hemorrhagic stroke [28,57], improves survival and function of nigral transplants in a rat model of Parkinson's disease [26], and partially rescues from mitochondrial dysfunction a Parkinson's disease model in *Caenorhabditis elegans* [58]. Additionally, TUDCA modulates Aβ-induced neuronal death by inhibiting the mitochondrial machinery and enhancing survival signaling [30], most likely through functional modulation of nuclear steroid receptors [32]. In particular, TUDCA was shown to mitigate primary neuron mitochondrial insufficiency and toxicity by inhibiting Bax translocation from cytosol to mitochondria [59] and subsequent downstream events ending in caspase activation, substrate cleavage and ultimately cell death. In this study, we show that TUDCA additionally protects brain microvascular endothelial cells from the apoptotic insult triggered by the potent vasculotropic E22Q peptide through suppression of Bax translocation, cytochrome *c* release and subsequent cell death. Notably, despite its potent anti-apoptotic role, TUDCA pre-treatment did not significantly alter the aggregation properties, fibrillogenic capacity or secondary structure of the Aβ peptides in our experimental *in vitro* paradigm. Future experiments should clarify whether TUDCA has any differential effect in the peptide fibrillization occurring in cell culture conditions.

The present data highlight a dichotomy between aggregation/fibrillization patterns and apoptotic properties of Aβ peptides in HCECs. Whether these observations downplay the role of high molecular mass structural assemblies in the induction of apoptosis, or simply indicate that TUDCA directly affects upstream pathways remains to be elucidated. It is conceivable that TUDCA may bind to the monomers/small oligomers of the Aβ peptides, affecting their capability to insert into lipid bilayers and form channels [60,61]. Alternatively, as a cholesterol-derived molecule, TUDCA may insert into cellular membranes [62,63], thus preventing the subsequent insertion of Aβ. Certainly, further studies are needed to identify the exact targets of TUDCA; nevertheless, this work provides new perspectives for the modulation of amyloid-induced toxicity in CAA, presenting new targets for therapeutic interventions.

Acknowledgements

This work was supported by grant PTDC/BIA-BCM/67922/2006 from Fundação para a Ciência e a Tecnologia (FCT), Lisbon, Portugal; NIH grants NS051715 andAG10491; and the American Heart Association. R.J.S.V. is the recipient of a PhD fellowship from FCT, Portugal (BD/30467/2006); A.F.N., R.E.C. and R.M.R. are recipients of postdoctoral fellowships from FCT, Portugal (BPD/34603/2007, BPD/30257/2006 and BPD/40623/2007, respectively).

References

1. Rensink AA, de Waal RM, Kremer B, Verbeek MM. Pathogenesis of cerebral amyloid angiopathy. Brain Res. Brain Res. Rev 2003;43:207–223. [PubMed: 14572915]
2. Coria F, Rubio I. Cerebral amyloid angiopathies. Neuropathol. Appl. Neurobiol 1996;22:216–227. [PubMed: 8804023]
3. Vinters HV. Cerebral amyloid angiopathy. A critical review. Stroke 1987;18:311–324. [PubMed: 3551211]
4. Yamada M. Cerebral amyloid angiopathy: an overview. Neuropathology 2000;20:8–22. [PubMed: 10935432]
5. Revesz T, Ghiso J, Lashley T, Plant G, Rostagno A, Frangione B, Holton JL. Cerebral amyloid angiopathies: a pathologic, biochemical and genetic view. J. Neuropathol. Exp. Neurol 2003;62:885–898. [PubMed: 14533778]
6. Ghiso J, Frangione B. Amyloidosis and Alzheimer's disease. Adv. Drug Deliv. Rev 2002;54:1539–1551. [PubMed: 12453671]
7. Selkoe D. Translating cell biology into therapeutic advances in Alzheimer's disease. Nature 1999;399:23–31.
8. Levy E, Carman MD, Fernandez-Madrid IJ, Power MD, Lieberburg I, van Duinen SG, Bots GT, Luyendijk W, Frangione B. Mutation of the Alzheimer's disease amyloid gene in hereditary cerebral hemorrhage, Dutch type. Science 1990;248:1124–1126. [PubMed: 2111584]
9. Miravalle L, Tokuda T, Chiarle R, Giaccone G, Bugiani O, Tagliavini F, Frangione B, Ghiso J. Substitutions at codon 22 of Alzheimer's abeta peptide induce diverse conformational changes and apoptotic effects in human cerebral endothelial cells. J. Biol. Chem 2000;275:27110–27116. [PubMed: 10821838]
10. Hendriks L, van Duijn CM, Cras P, Cruts M, Van Hul W, van Harskamp F, Warren A, McInnis MG, Antonarakis SE, Martin JJ, et al. Presenile dementia and cerebral haemorrhage linked to a mutation at codon 692 of the beta-amyloid precursor protein gene. Nat. Genet 1992;1:218–221. [PubMed: 1303239]
11. Grabowski TJ, Cho HS, Vonsattel JP, Rebeck GW, Greenberg SM. Novel amyloid precursor protein mutation in an Iowa family with dementia and severe cerebral amyloid angiopathy. Ann. Neurol 2001;49:697–705. [PubMed: 11409420]
12. Zhang-Nunes SX, Maat-Schieman ML, van Duinen SG, Roos RA, Frosch MP, Greenberg SM. The cerebral beta-amyloid angiopathies: hereditary and sporadic. Brain Pathol 2006;16:30–39. [PubMed: 16612980]
13. Maat-Schieman ML, Yamaguchi H, van Duinen SG, Natte R, Roos RA. Age-related plaque morphology and C-terminal heterogeneity of amyloid beta in Dutch-type hereditary cerebral hemorrhage with amyloidosis. Acta Neuropathol 2000;99:409–419. [PubMed: 10787040]
14. Natte R, Maat-Schieman ML, Haan J, Bornebroek M, Roos RA, van Duinen SG. Dementia in hereditary cerebral hemorrhage with amyloidosis-Dutch type is associated with cerebral amyloid angiopathy but is independent of plaques and neurofibrillary tangles. Ann. Neurol 2001;50:765–772. [PubMed: 11761474]
15. Maat-Schieman M, Roos R, van Duinen S. Hereditary cerebral hemorrhage with amyloidosis-Dutch type. Neuropathology 2005;25:288–297. [PubMed: 16382777]
16. Murakami K, Irie K, Morimoto A, Ohigashi H, Shindo M, Nagao M, Shimizu T, Shirasawa T. Neurotoxicity and physicochemical properties of Abeta mutant peptides from cerebral amyloid angiopathy: implication for the pathogenesis of cerebral amyloid angiopathy and Alzheimer's disease. J. Biol. Chem 2003;278:46179–46187. [PubMed: 12944403]
17. Van Nostrand WE, Melchor JP, Cho HS, Greenberg SM, Rebeck GW. Pathogenic effects of D23N Iowa mutant amyloid beta-protein. J. Biol. Chem 2001;276:32860–32866. [PubMed: 11441013]
18. Davis J, Van Nostrand WE. Enhanced pathologic properties of Dutch-type mutant amyloid beta-protein. Proc. Natl. Acad. Sci. USA 1996;93:2996–3000. [PubMed: 8610157]
19. Eisenhauer PB, Johnson RJ, Wells JM, Davies TA, Fine RE. Toxicity of various amyloid beta peptide species in cultured human blood-brain barrier endothelial cells: increased toxicity of dutch-type mutant. J. Neurosci. Res 2000;60:804–810. [PubMed: 10861793]

20. Wisniewski T, Ghiso J, Frangione B. Peptides homologous to the amyloid protein of Alzheimer's disease containing a glutamine for glutamic acid substitution have accelerated amyloid fibril formation. Biochem. Biophys. Res. Commun 1991;179:1247–1254. [PubMed: 1681804]
21. Nilsberth C, Westlind-Danielsson A, Eckman CB, Condron MM, Axelman K, Forsell C, Stenh C, Luthman J, Teplow DB, Younkin SG, et al. The 'Arctic' APP mutation (E693G) causes Alzheimer's disease by enhanced Abeta protofibril formation. Nat. Neurosci 2001;4:887–893. [PubMed: 11528419]
22. Klyubin I, Walsh DM, Cullen WK, Fadeeva JV, Anwyl R, Selkoe DJ, Rowan MJ. Soluble Arctic amyloid beta protein inhibits hippocampal long-term potentiation *in vivo*. Eur. J. Neurosci 2004;19:2839–2846. [PubMed: 15147317]
23. Paris D, Ait-Ghezala G, Mathura VS, Patel N, Quadros A, Laporte V, Mullan M. Anti-angiogenic activity of the mutant Dutch A(beta) peptide on human brain micro-vascular endothelial cells. Brain Res. Mol. Brain Res 2005;136:212–230. [PubMed: 15893605]
24. Rodrigues CMP, Fan G, Ma X, Kren BT, Steer CJ. A novel role for ursodeoxycholic acid in inhibiting apoptosis by modulating mitochondrial membrane perturbation. J. Clin. Invest 1998;101:2790–2799. [PubMed: 9637713]
25. Macedo B, Batista AR, Ferreira N, Almeida MR, Saraiva MJ. Anti-apoptotic treatment reduces transthyretin deposition in a transgenic mouse model of Familial Amyloidotic Polyneuropathy. Biochim. Biophys. Acta 2008;1782:517–522. [PubMed: 18572024]
26. Duan WM, Rodrigues CMP, Zhao LR, Steer CJ, Low WC. Tauroursodeoxycholic acid improves the survival and function of nigral transplants in a rat model of Parkinson's disease. Cell Transplant 2002;11:195–205. [PubMed: 12075985]
27. Keene CD, Rodrigues CMP, Eich T, Chhabra MS, Steer CJ, Low WC. Tauroursodeoxycholic acid, a bile acid, is neuroprotective in a transgenic animal model of Huntington's disease. Proc. Natl. Acad. Sci. USA 2002;99:10671–10676. [PubMed: 12149470]
28. Rodrigues CMP, Solá S, Nan Z, Castro RE, Ribeiro PS, Low WC, Steer CJ. Tauroursodeoxycholic acid reduces apoptosis and protects against neurological injury after acute hemorrhagic stroke in rats. Proc. Natl. Acad. Sci. USA 2003;100:6087–6092. [PubMed: 12721362]
29. Colak A, Kelten B, Sagmanligil A, Akdemir O, Karaoglan A, Sahan E, Celik O, Barut S. Tauroursodeoxycholic acid and secondary damage after spinal cord injury in rats. J. Clin. Neurosci 2008;15:665–671. [PubMed: 18343118]
30. Solá S, Castro RE, Laires PA, Steer CJ, Rodrigues CMP. Tauroursodeoxycholic acid prevents amyloid-beta peptide-induced neuronal death via a phosphatidylinositol 3-kinase-dependent signaling pathway. Mol. Med 2003;9:226–234. [PubMed: 15208744]
31. Ramalho RM, Ribeiro PS, Solá S, Castro RE, Steer CJ, Rodrigues CMP. Inhibition of the E2F-1/p53/Bax pathway by tauroursodeoxycholic acid in amyloid beta-peptide-induced apoptosis of PC12 cells. J. Neurochem 2004;90:567–575. [PubMed: 15255934]
32. Solá S, Amaral JD, Borralho PM, Ramalho RM, Castro RE, Aranha MM, Steer CJ, Rodrigues CMP. Functional modulation of nuclear steroid receptors by tauroursodeoxycholic acid reduces amyloid beta-peptide-induced apoptosis. Mol. Endocrinol 2006;20:2292–2303. [PubMed: 16728529]
33. Ghiso J, Shayo M, Calero M, Ng D, Tomidokoro Y, Gandy S, Rostagno A, Frangione B. Systemic catabolism of Alzheimer's Abeta40 and Abeta42. J. Biol. Chem 2004;279:45897–45908. [PubMed: 15322125]
34. Dahlgren KN, Manelli AM, Stine WB Jr, Baker LK, Krafft GA, LaDu MJ. Oligomeric and fibrillar species of amyloid-beta peptides differentially affect neuronal viability. J. Biol. Chem 2002;277:32046–32053. [PubMed: 12058030]
35. Kelly SM, Jess TJ, Price NC. How to study proteins by circular dichroism. Biochim. Biophys. Acta 2005;1751:119–139. [PubMed: 16027053]
36. Walsh DM, Hartley DM, Kusumoto Y, Fezoui Y, Condron MM, Lomakin A, Benedek GB, Selkoe DJ, Teplow DB. Amyloid beta-protein fibrillogenesis. Structure and biological activity of protofibrillar intermediates. J. Biol. Chem 1999;274:25945–25952. [PubMed: 10464339]
37. LeVine H 3rd. Quantification of beta-sheet amyloid fibril structures with thioflavin T. Methods Enzymol 1999;309:274–284. [PubMed: 10507030]

38. Shin Y, Cho HS, Fukumoto H, Shimizu T, Shirasawa T, Greenberg SM, Rebeck GW. Abeta species, including IsoAsp23 Abeta, in Iowa-type familial cerebral amyloid angiopathy. Acta Neuropathol 2003;105:252–258. [PubMed: 12557012]
39. Castano EM, Prelli F, Soto C, Beavis R, Matsubara E, Shoji M, Frangione B. The length of amyloid-beta in hereditary cerebral hemorrhage with amyloidosis, Dutch type. Implications for the role of amyloid-beta 1–42 in Alzheimer's disease. J. Biol. Chem 1996;271:32185–32191. [PubMed: 8943274]
40. Kumar-Singh S, Cras P, Wang R, Kros JM, van Swieten J, Lübke U, Ceuterick C, Serneels S, Vennekens K, Timmermans JP, et al. Dense-core senile plaques in the Flemish variant of Alzheimer's disease are vasocentric. Am. J. Pathol 2002;161:507–520. [PubMed: 12163376]
41. Mori H, Takio K, Ogawara M, Selkoe DJ. Mass spectrometry of purified amyloid beta protein in Alzheimer's disease. J. Biol. Chem 1992;267:17082–17086. [PubMed: 1512246]
42. Miller DL, Papayannopoulos IA, Styles J, Bobin SA, Lin YY, Biemann K, Iqbal K. Peptide compositions of the cerebrovascular and senile plaque core amyloid deposits of Alzheimer's disease. Arch. Biochem. Biophys 1993;301:41–52. [PubMed: 8442665]
43. Caughey B, Lansbury PT. Protofibrils, pores, fibrils and neurodegeneration: separating the responsible protein aggregates from the innocent bystanders. Annu. Rev. Neurosci 2003;26:267–298. [PubMed: 12704221]
44. Walsh DM, Selkoe DJ. A beta oligomers – a decade of discovery. J. Neurochem 2007;101:1172–1184. [PubMed: 17286590]
45. McLean CA, Cherny RA, Fraser FW, Fuller SJ, Smith MJ, Beyreuther K, Bush AI, Masters CL. Soluble pool of Abeta amyloid as a determinant of severity of neurodegeneration in Alzheimer's disease. Ann. Neurol 1999;46:860–866. [PubMed: 10589538]
46. Lue LF, Kuo YM, Roher AE, Brachova L, Shen Y, Sue L, Beach T, Kurth JH, Rydel RE, Rogers J. Soluble amyloid beta peptide concentration as a predictor of synaptic change in Alzheimer's disease. Am. J. Pathol 1999;155:853–862. [PubMed: 10487842]
47. Whalen BM, Selkoe DJ, Hartley DM. Small non-fibrillar assemblies of amyloid beta-protein bearing the Arctic mutation induce rapid neuritic degeneration. Neurobiol. Dis 2005;20:254–266. [PubMed: 16242634]
48. Ma B, Nussinov R. The stability of monomeric intermediates controls amyloid formation:Abeta25–35 and its N27Q mutant. Biophys. J 2006;90:3365–3374. [PubMed: 16500972]
49. Zheng J, Jang H, Ma B, Tsai CJ, Nussinov R. Modeling the Alzheimer Abeta17–42 fibril architecture: tight intermolecular sheet-sheet association and intramolecular hydrated cavities. Biophys. J 2007;93:3046–3057. [PubMed: 17675353]
50. Lazo ND, Grant MA, Condron MC, Rigby AC, Teplow DB. On the nucleation of amyloid beta-protein monomer folding. Protein Sci 2005;14:1581–1596. [PubMed: 15930005]
51. Grant MA, Lazo ND, Lomakin A, Condron MM, Arai H, Yamin G, Rigby AC, Teplow DB. Familial Alzheimer's disease mutations alter the stability of the amyloid beta-protein monomer folding nucleus. Proc. Natl. Acad. Sci. USA 2007;104:16522–16527. [PubMed: 17940047]
52. Krone MG, Baumketner A, Bernstein SL, Wyttenbach T, Lazo ND, Teplow DB, Bowers MT, Shea JE. Effects of familial Alzheimer's disease mutations on the folding nucleation of the amyloid beta-protein. J. Mol. Biol 2008;381:221–228. [PubMed: 18597778]
53. Youle RJ, Strasser A. The BCL-2 protein family: opposing activities that mediate cell death. Nat. Rev. Mol. Cell Biol 2008;9:47–59. [PubMed: 18097445]
54. Mattson MP. Apoptosis in neurodegenerative disorders. Nat. Rev. Mol. Cell Biol 2000;1:120–129. [PubMed: 11253364]
55. Sajan FD, Martiniuk F, Marcus DL, Frey WH 2nd, Hite R, Bordayo EZ, Freedman ML. Apoptotic gene expression in Alzheimer's disease hippocampal tissue. Am. J. Alzheimers Dis. Other Demen 2007;22:319–328. [PubMed: 17712163]
56. Keene CD, Rodrigues CMP, Eich T, Linehan-Stieers C, Abt A, Kren BT, Steer CJ, Low WC. A bile acid protects against motor and cognitive deficits and reduces striatal degeneration in the 3-nitropropionic acid model of Huntington's disease. Exp. Neurol 2001;171:351–360. [PubMed: 11573988]

57. Rodrigues CMP, Spellman SR, Solá S, Grande AW, Linehan-Stieers C, Low WC, Steer CJ. Neuroprotection by a bile acid in an acute stroke model in the rat. J. Cereb. Blood Flow Metab 2002;22:463–471. [PubMed: 11919517]
58. Ved R, Saha S, Westlund B, Perier C, Burnam L, Sluder A, Hoener M, Rodrigues CMP, Alfonso A, Steer C, et al. Similar patterns of mitochondrial vulnerability and rescue induced by genetic modification of alpha-synuclein, parkin, and DJ-1 in *Caenorhabditis elegans*. J. Biol. Chem 2005;280:42655–42668. [PubMed: 16239214]
59. Rodrigues CMP, Stieers CL, Keene CD, Ma X, Kren BT, Low WC, Steer CJ. Tauroursodeoxycholic acid partially prevents apoptosis induced by 3-nitropropionic acid: evidence for amitochondrial pathway independent of the permeability transition. J. Neurochem 2000;75:2368–2379. [PubMed: 11080188]
60. Jang H, Zheng J, Lal R, Nussinov R. New structures help the modeling of toxic amyloidbeta ion channels. Trends Biochem. Sci 2008;33:91–100. [PubMed: 18182298]
61. Jang H, Zheng J, Nussinov R. Models of beta-amyloid ion channels in the membrane suggest that channel formation in the bilayer is a dynamic process. Biophys. J 2007;93:1938–1949. [PubMed: 17526580]
62. Guldutuna S, Zimmer G, Imhof M, Bhatti S, You T, Leuschner U. Molecular aspects of membrane stabilization by ursodeoxycholate. Gastroenterology 1993;104:1736–1744. [PubMed: 8388838]
63. Rodrigues CMP, Solá S, Sharpe JC, Moura JJ, Steer CJ. Tauroursodeoxycholic acid prevents Bax-induced membrane perturbation and cytochrome C release in isolated mitochondria. Biochemistry 2003;42:3070–3080. [PubMed: 12627974]

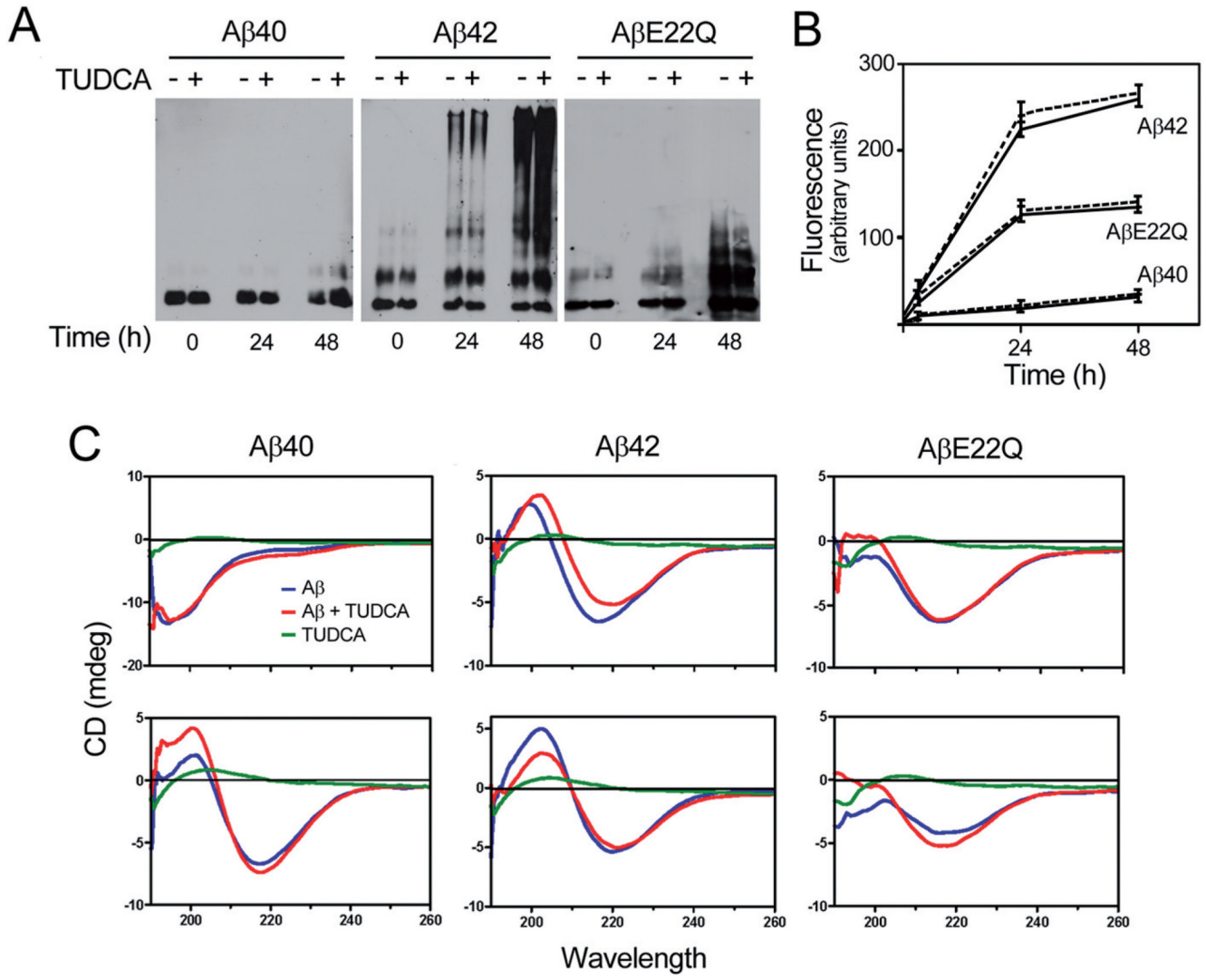

Figure 1.

Structural studies of wild-type and Dutch-variant Aβ peptides. HFIP-treated peptides at 1 mg/ml in PBS were aggregated at 37°C for up to 48 h. Peptide aggregation/fibrillization propensity as well as secondary structure were analyzed both in the presence and absence of 100 μMTUDCA. (*a*) Oligomerization of wild-type and Dutch-variant peptides assessed by Western blot probed with a combination of monoclonal anti-Aβ antibodies 4G8 and 6E10 after separation on 16.5% Tris-Tricine SDS-PAGE. (*b*) Fibrillization of wild-type and Dutch-variant peptides estimated by fluorescence evaluation (excitation/emission wavelengths 435 nm/490 nm, respectively) after Thioflavin T binding. Solid lines, Aβ peptides alone; broken lines, Aβ peptides in the presence of TUDCA. (*c*) Secondary structure of wild-type and Dutch-variant peptides assessed through the respective spectra in the far-UV light (190–260 nm) in a Jasco J-720 spectropolarimeter via a 0.2 mm-path quartz cell, at 24 (top) and 48 h (bottom) of aggregation. Blue, Aβ peptides alone; red, Aβ peptides in the presence of TUDCA; green, TUDCA alone.

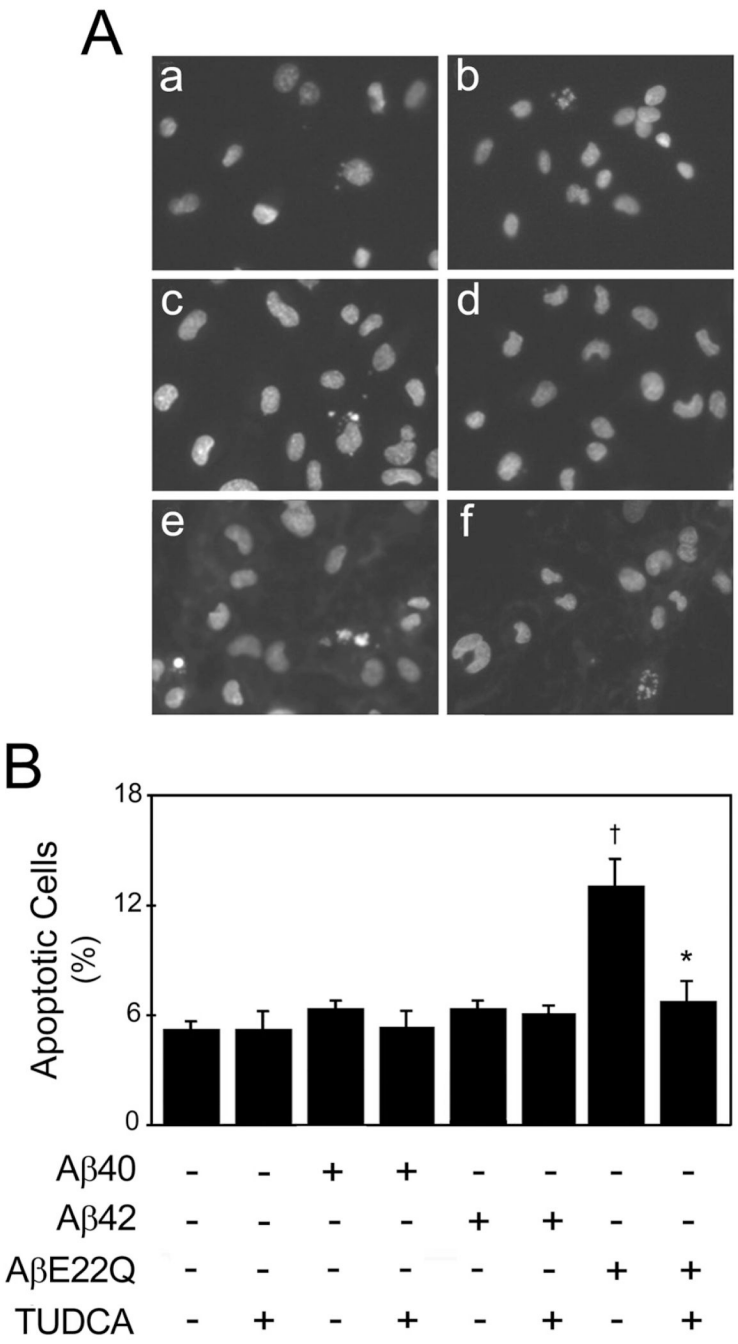

Figure 2.

AβE22Q-induced apoptosis in HCECs is inhibited by TUDCA. Cells were incubated either with vehicle (control), 50 μM of wild-type or Dutch-variant Aβ peptides, ± 100 μMTUDCA for 24 h. In co-incubation experiments, cells were pre-treated with TUDCA for 12 h and the bile acid was left in the culture medium with Aβ peptides. (*a*) Fluorescence microscopy of Hoechst staining shows condensed or fragmented nuclei indicative of apoptosis in control cells (a), and in cells exposed to TUDCA (b), Aβ40 (c) and Aβ42 (d). Nuclear condensation or fragmentation was markedly increased in cells incubated with AβE22Q (e), but less evident in cells exposed to AβE22Q plus TUDCA (f). (*b*) Histogram shows the percentage of apoptotic cells (mean ± SEM) identified by condensed and fragmented chromatin contiguous to the

nuclear membrane, as well as nuclear fragmentation and presence of apoptotic bodies, following Hoechst staining and fluorescence microscopy. †$p<0.001$ from control; *$p<0.05$ from AβE22Q.

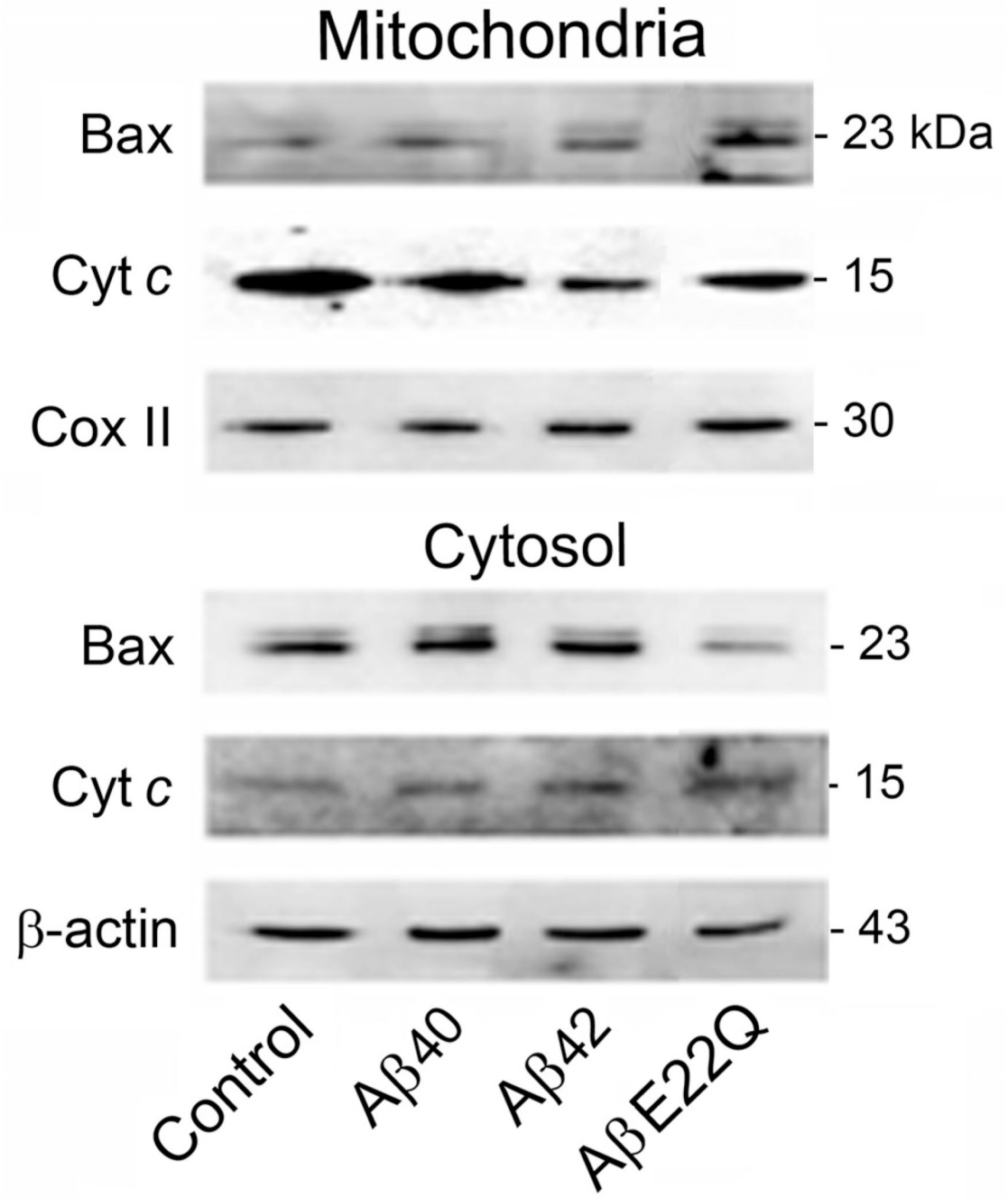

Figure 3.

AβE22Q-induced Bax translocation and cytochrome *c* release in HCECs. Cells were incubated either with vehicle (control), or 50 μM wild-type or Dutch-variant Aβ peptides for 24 h. Mitochondrial and cytosolic protein fractions were extracted for Western blot analysis. Representative immunoblots of Bax and cytochrome *c* cellular distribution are shown. Cytochrome *c* oxidase II (Cox II) and β-actin were used as loading controls for mitochondrial and cytosolic fractions, respectively. Cyt *c*, cytochrome *c*.

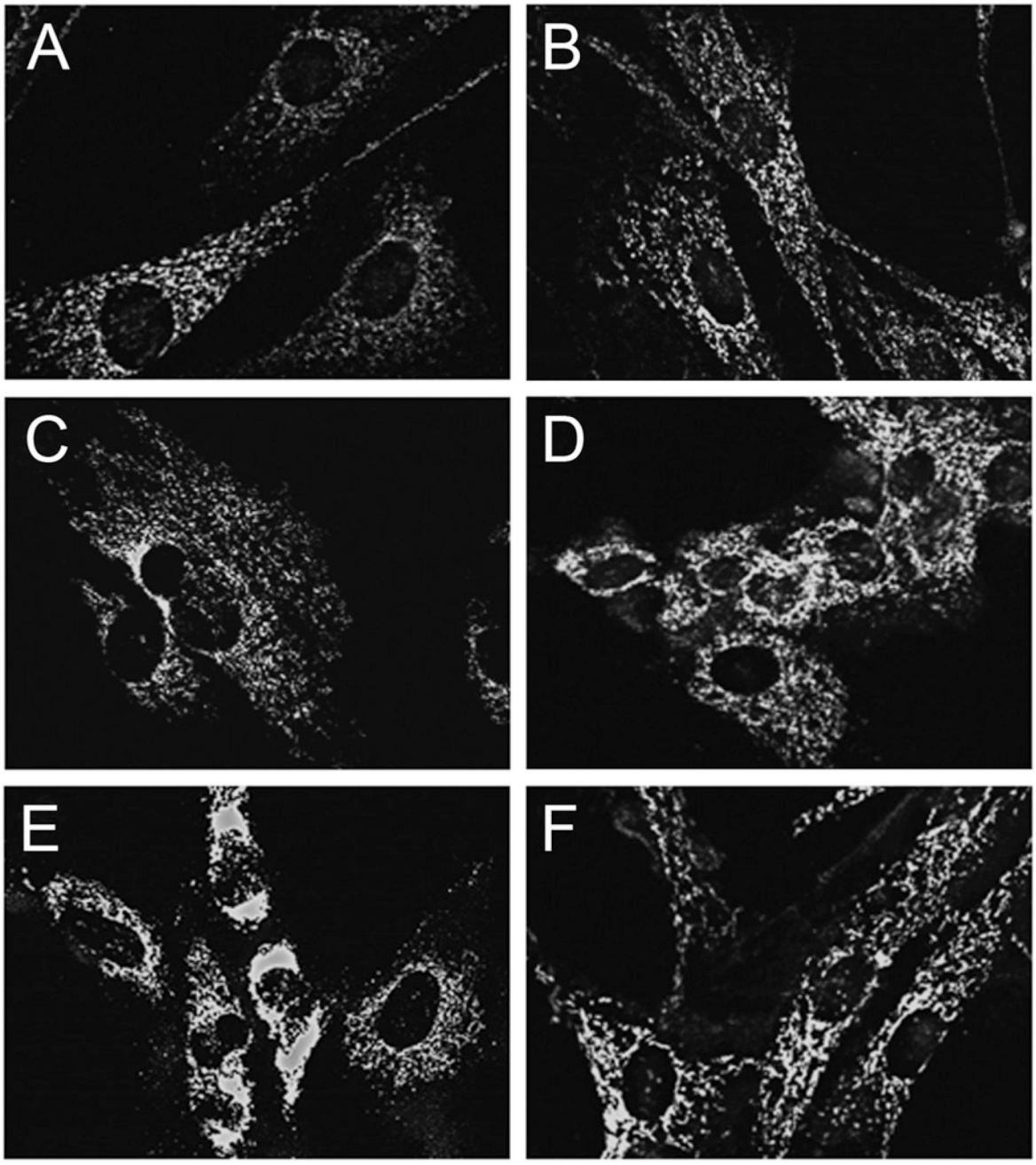

Figure 4.
TUDCA inhibits AβE22Q-induced cytochrome *c* release in HCECs. Cells were incubated either with vehicle (control), 50 μM of wild-type or Dutch-variant Aβ peptides, ± 100 μM TUDCA for 24 h. In co-incubation experiments, cells were pretreated with TUDCA for 12 h and the bile acid was left in the culture medium with Aβ peptides. Fluorescence microscopy shows mitochondrial localization of cytochrome *c* in control cells (a) and in cells exposed to TUDCA (b), Aβ40 (c) and Aβ42 (d). Strong cytoplasmic staining was evident in cells incubated with AβE22Q (e). Notably, co-incubation with TUDCA mostly abolished the effect induced by the Dutch-variant peptide (f).

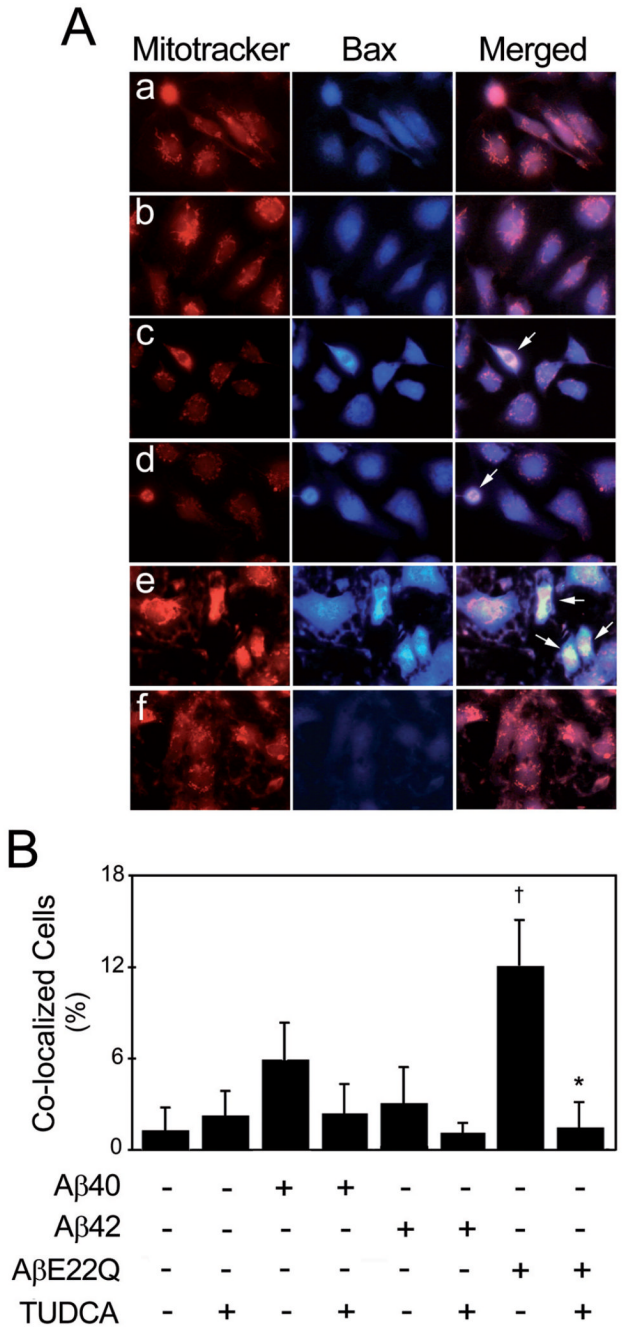

Figure 5.

TUDCA inhibits AβE22Q-induced Bax translocation to the mitochondria in HCECs. Cells were incubated either with vehicle (control), 50 μM of wild-type or Dutch-variant Aβ peptides, ± 100 μM TUDCA for 24 h. In co-incubation experiments, cells were pre-treated with TUDCA for 12 h and the bile acid was left in the culture medium with Aβ peptides. (*a*) Fluorescence microscopy shows co-localization of Bax (in blue) with the mitochondria (in red) in control cells (a), and in cells exposed to TUDCA (b), Aβ40 (c) and Aβ42 (d). Mitochondrial co-localization of Bax was markedly increased in cells incubated with AβE22Q (e), but less evident in cells exposed to AβE22Q plus TUDCA (f). (*b*) Histogram shows mean ± SEM percentage of co-localized cells. †$p<0.05$ from control; *$p<0.05$ from AβE22Q.